Ionosphere Effects for Wideband GNSS Signals

Grace Xingxin Gao, Seebany Datta-Barua, Todd Walter, and Per Enge
Stanford University

BIOGRAPHY

Grace Xingxin Gao is a Ph.D. candidate under the guidance of Professor Per Enge in the Electrical Engineering Department at Stanford University. She received a B.S. in Mechanical Engineering in 2001 and her M.S. in Electrical Engineering in 2003, at Tsinghua University, Beijing, China. Her current research interests include Galileo signal and code structures, GNSS receiver architectures, and GPS modernization.

Seebany Datta-Barua is a Ph.D. candidate under the guidance of Professor Per Enge and Dr. Todd Walter in the Aeronautics and Astronautics Department at Stanford University. She received a B.S. in Physics with a Minor in Mathematics in 2000 and her M.S. in Aeronautics and Astronautics in 2002, also at Stanford. Her current research interests lie in the study of mid-latitude space weather as it pertains to the integrity and availability of GPS-based augmentation systems.

Todd Walter is a Senior Research Engineer in the Department of Aeronautics and Astronautics at Stanford University. Dr. Walter received his PhD. in 1993 from Stanford and is currently developing WAAS integrity algorithms and analyzing the availability of the WAAS signal. He is a fellow of the ION.

Per Enge is a Professor of Aeronautics and Astronautics at Stanford University, where he is the Kleiner-Perkins, Mayfield, Sequoia Capital Professor in the School of Engineering. He directs the GPS Research Laboratory, which develops satellite navigation systems based on the Global Positioning System (GPS). He has been involved in the development of WAAS and LAAS for the FAA. Per has received the Kepler, Thurlow and Burka Awards from the ION for his work. He is also a Fellow of the ION and the Institute of Electrical and Electronics Engineers (IEEE). He received his Ph.D. from the University of Illinois in 1983.

ABSTRACT

Wideband signals show promise for Galileo development and GPS modernization because they provide sharper correlation peaks and thus more accuracy. For instance, the Galileo E5 signal occupies the frequency band from 1164 MHz to 1215 MHz, over 25 times the two-sided bandwidth of the GPS C/A code. However, because the ionosphere is dispersive, different frequency components in the wideband spectrum suffer different delays as they traverse the upper atmosphere.

Signal delay due to refraction through the ionosphere is the largest and most variable source of positioning error for single frequency receivers. There are many models to compensate for the ionospheric delay. A classic and well-known formula is the first-order ionospheric delay model, in which the excess group delay is inversely proportional to frequency squared. Dual frequency receivers take advantage of this to compensate for the ionosphere errors by assuming each incoming signal to be a single frequency tone represented by the center frequency. This simplification is effective for narrowband signals, such as the GPS L1 C/A code, whose two-sided bandwidth is only 2 MHz. As the frequency band gets wider, the ionospheric delay variation within the band becomes larger. Thus, we should no longer neglect it as in the narrowband signal case. This motivates us to update the ionosphere model to take into account all frequency elements of the GNSS signals rather than treating them as a single tone.

In this paper, we demonstrate the method of calculating ionospheric delay of wideband signals. We first decompose the time domain signal into the frequency domain, apply variable delays to all the frequency components, then transfer the frequency domain signal back to the time domain. The model modifies the total group delay of wideband signals. Moreover, it captures another ionosphere effect, signal deformation, which is not captured by the classical model. A signal traveling through the ionosphere becomes distorted due to varying delay over its bandwidth. We neglect frequency-dependent bending of the signal.

We also apply the method to a variety of wideband signals, the Galileo E5b signal, the Galileo E5 signal, and BPSK signals with a range of bandwidths. The simulation results show the ionosphere impact on time-domain signal deformation, power loss of the correlation peak, phase shift in the PLL output, correlation peak

symmetry and the frequency spectrum. Throughout the remainder of the paper, "bandwidth" refers to the two-sided bandwidth of a signal.

INTRODUCTION

The Galileo Navigation Signal-in-Space Interface Control Document (SIS ICD) [1] specifies the frequency plan of the GIOVE-A signals as shown in Figure 1. The frequency bands are E5 (with subbands of E5a and E5b), E6, and L1 bands. The two-sided bandwidths of these Galileo signals are listed in Table 1. Galileo signals are allocated with wide frequency bands. For instance, the Galileo E5 signal band is 51.150 MHz, over 25 times the bandwidth of the GPS C/A code.

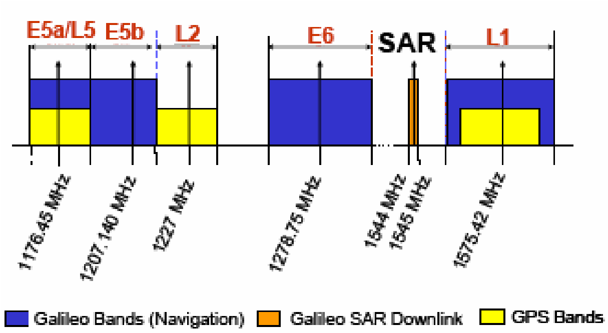

Figure 1: Frequency plan of GIOVE-A signals

Signal Rx Reference Bandwidth
E5 51.150 MHz [E5a 20.460 MHz] [E5b 20.460 MHz]
E6 40.920 MHz
L1 32.736 MHz

Table 1: GIOVE-A Navigation SIS Rx Reference Bandwidth

The ionosphere is dispersive; different frequency components in the wideband spectrum suffer different delays as they traverse the upper atmosphere. Based on the first-order ionospheric delay model [3], the excess group delay in meters is expressed as:

$$\tau(f) = \frac{40.3TEC}{f^2} \qquad \text{Eq. (1),}$$

where TEC is the total electron content (electrons/m^2) and f (Hz) is the frequency of the transmitted signal. For narrowband signals, such as the 2 MHz GPS C/A code, the ionospheric delay within the signal frequency band does not vary much. Thus, the signal can be considered as a single frequency tone represented by the center frequency. As the frequency band gets wider, the ionospheric delay variation within the band becomes larger. Figure 2 shows how the delay varies as a function of frequency relative to a center frequency of 1.2 GHz. The delay is neither constant nor linear over the frequency band. Moreover, it is asymmetric. Considering a 500 MHz signal centered at 1.2 GHz, the lower end of the band has 14 m more ionospheric delay with respect to the delay at the center frequency. On contrast, the higher end of the band has 8 m less delay. A variation of 22 m over a 500 MHz band indicates that we should consider the bandwidth effect when calculating ionospheric delay for wideband GNSS signals.

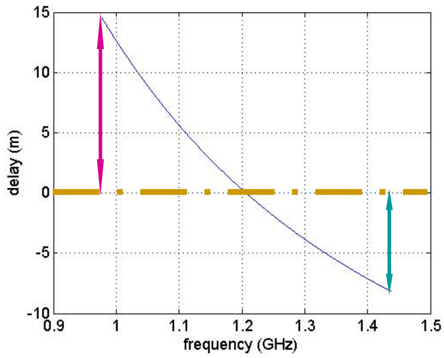

Figure 2: Ionospheric delay with respect to frequency

The ionosphere effect for general wideband signals was brought up and studied in [2]. This paper will focus on Galileo signals and simulated BPSK signals with different bandwidths. The first section of the paper provides the method for calculating wideband ionosphere effect. The second section studies the ionosphere effect on the Galileo E5b signal, including time-domain signal deformation and correlation function degradation. The third section simulates the Galileo E5 signal. It has Alternate Binary Offset Carrier (AltBOC) modulation and contains both E5a and E5b signals. The E5 signal has 2.5 times the bandwidth of the E5b signal by itself. The simulation results show more pronounced ionosphere impact on the E5 signal than E5b signal only. The Galileo E5 signals with different Total Electron Content (TEC) values are also simulated. Finally, BPSK signals with different bandwidths and different TEC values are studied to evaluate the combined impact of bandwidth and TEC values.

WIDEBAND IONOSPHERE EFFECT

In order to calculate the wideband ionosphere effect, we assume the signal at the transmitter is $S(t)$. As the ionospheric delay is frequency dependent, we first convert $S(t)$ into the frequency domain by using the Fast Fourier Transform (FFT). The signal is then decomposed into different frequency components. Each frequency component suffers a corresponding ionospheric delay as a function of the frequency, denoted $\tau(f)$ as given in Equation (1). According to the first order ionosphere model, $\tau(f)$ can be expressed in Equation (2). As a delay in the time domain is equivalent to a phase shift in the frequency domain, the phase shift is then applied to each frequency component to obtain the frequency representation of the signal after passing through the ionosphere. The time-domain signal $S_{iono}(t)$ of the wideband signal after passage through the ionosphere is obtained by transforming the frequency-domain counterparts by Inverse Fast Fourier Transform (IFFT), as expressed in Equation (2). Combining Equation (1) and Equation (2), the signal with wideband ionosphere effect can be also written as in Equation (3). The procedure for calculating the wideband ionosphere effect is illustrated in Figure 3.

$$S_{iono}(t) = ifft\{ fft\{S(t)\} \cdot e^{-j2\pi \cdot f \cdot \tau(f)} \} \qquad \text{Eq. (2)}$$

eq. (2)

$$S_{iono}(t) = \int_{-\infty}^{\infty} \left(\int_{-\infty}^{\infty} S(t) \cdot e^{-j2\pi \cdot f \cdot t} dt \right) \cdot e^{-j2\pi \cdot (40.3 \cdot TEC / f - f \cdot t)} df$$

Eq. (3)

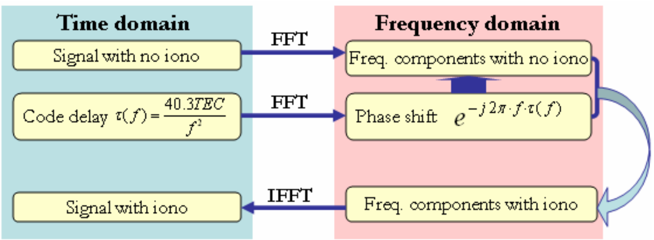

Figure 3: Calculating ionosphere effects for wideband signals

In the following sections, we will study the ionosphere effect for the Galileo E5b signal, E5 signal and the simulated BPSK signal in E5 band and with different bandwidths by using the above theory.

GALILEO E5B SIGNAL

We first study the ionosphere effect on the Galileo E5b signal. According to the Galileo SIS ICD [1], the broadcast E5b signal is a Binary Phase Shift Keying (BPSK) signal at a center frequency of 1207.14 MHz with a chip rate 10.23 Mcps. The Pseudo-Random Noise (PRN) codes of the current GIOVE-A broadcasting signals are decoded and the code generators are derived in [4]. In this section, we use the GIOVE-A E5b codes to simulate the Galileo E5b signal. For simplicity, we only show the inphase channel signal. We take TEC=100 TECU (TEC Unit) for the simulation. This is a typical midlatitude daytime value and corresponds to a delay of about 13 m for GPS L1 frequency users.

The power spectral density of the simulated baseband E5b signal features a main lobe in the middle and side lobes as shown in Figure 4. The ionosphere does not affect the shape of the signal spectrum because the time-domain delays of each frequency component due to the ionosphere are converted to phase shifts in the frequency domain. Thus, the ionosphere affects the phase, but not amplitude of the frequency-domain representation. The spectrum of the wideband signal remains the same before and after refraction through the ionosphere.

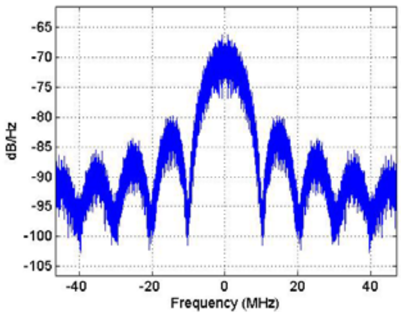

Figure 4: Power spectral density of the simulated E5b signal

Figure 5 shows time-domain E5b signals. We compare the assumptions of non-dispersive and dispersive ionosphere. In the first case, we ignore the signal bandwidth by assuming all frequency components have the same ionospheric delay at the center frequency f0. The real part of such a signal is shown in blue and the imaginary part in green. In the second case, the frequency components have different delays with respect to the corresponding frequencies. The ionosphere causes ripples in the real part of the signal (red). Moreover, it creates a nonzero imaginary part (cyan). Since the Phase Lock Loop (PLL) performs tracking by maximizing the energy in the in-phase channel and minimizing the quadrature channel energy, a nonzero imaginary signal results in a phase change at the PLL output.

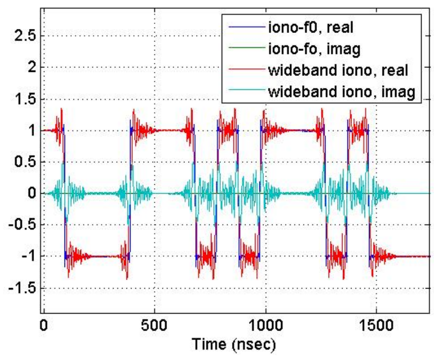

Figure 5: Time-domain E5b signals with ionosphere effect

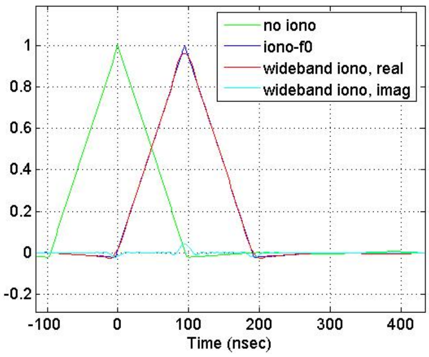

Figure 6: Correlation functions of Galileo E5b signal with and without ionospheric effect

The correlation functions are shown in Figure 6. The dispersive ionosphere does not have a significant impact. The correlation peak with dispersive ionosphere decreases 0.2dB and the phase at the PLL output is 3 degrees. The maximal early-minus-late discriminator output with the correlator spacing from 0 to 2 chips is only 1.2% of the correlation peak. The impact on the correlation peak is small for two reasons. First, correlation operates as a low-pass filter. It integrates the PRN code for 1 msec and thus smoothes out the ripples in the time-domain signal. Second, the Galileo E5b signal has bandwidth of 20 MHz, which is not wide enough to make the dispersive ionosphere effect significant.

GALILEO E5 SIGNAL

The Galileo E5 signal includes E5a and E5b signals. The full E5 signal has 2.5 times the bandwidth of E5b only. Sub-bands E5a and E5b are each 20 MHz BPSK signals centered at 1176.45 MHz and 1207.14 MHz, respectively. The E5 signal as a whole is an Alternate Binary Offset Code (AltBOC(15, 10)) signal centered at 1191.795 MHz [1]. According to the SIS ICD, there are two codes, E5a-I and E5a-Q in E5a band and another two codes, E5b-I and E5b-Q in E5b band. The I channels are the data channels and the Q channels are dataless pilot channels. The code chip rate is 10*1.023 Mcps; and the digital subcarrier frequency is 15*1.023 MHz. The E5 modulation is described in [5] and shown in Figure 7.

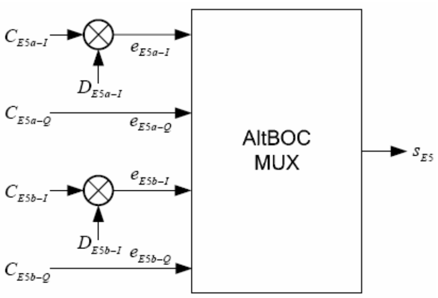

Figure 7: E5 modulation scheme

In Figure 7 C_{E5a-I}, C_{E5a-Q}, C_{E5b-I} and C_{E5b-Q} are binary E5 ranging codes as derived in [4]. D_{E5a-I} and D_{E5b-I} are binary navigation message bits. The resulting signals from the data-modulated ranging codes are e_{E5a-I}, e_{E5a-Q}, e_{E5b-I} and e_{E5b-Q} as expressed in Equation (4).

$$e_{E5a-I}(t) = \sum_{i=-\infty}^{+\infty}\left[c_{E5a-I,|i|_{L_{E5a-I}}} \cdot d_{E5a-I,[i]_{DC_{E5a-I}}}\, rect_{T_{C,E5a-I}}\left(t - i\cdot T_{C,E5a-I}\right)\right]$$
$$e_{E5a-Q}(t) = \sum_{i=-\infty}^{+\infty}\left[c_{E5a-Q,|i|_{L_{E5a-Q}}} \cdot rect_{T_{C,E5a-Q}}\left(t - i\cdot T_{C,E5a-Q}\right)\right]$$
$$e_{E5b-I}(t) = \sum_{i=-\infty}^{+\infty}\left[c_{E5b-I,|i|_{L_{E5b-I}}} \cdot d_{E5b-I,[i]_{DC_{E5b-I}}}\, rect_{T_{C,E5b-I}}\left(t - i\cdot T_{C,E5b-I}\right)\right]$$
$$e_{E5b-Q}(t) = \sum_{i=-\infty}^{+\infty}\left[c_{E5b-Q,|i|_{L_{E5b-Q}}} \cdot rect_{T_{C,E5b-Q}}\left(t - i\cdot T_{C,E5b-Q}\right)\right]$$

Eq. (4)

The output E5 signal is the modulated navigation signal with digital sub carriers as shown in Equation (5):

$$\begin{aligned} s_{E5}(t) = & \frac{1}{2\sqrt{2}}\left(e_{E5a-I}(t) + j\,e_{E5a-Q}(t)\right)\left[sc_{E5-S}(t) - j\,sc_{E5-S}\left(t - T_{s,E5}/4\right)\right] \\ & + \frac{1}{2\sqrt{2}}\left(e_{E5b-I}(t) + j\,e_{E5b-Q}(t)\right)\left[sc_{E5-S}(t) + j\,sc_{E5-S}\left(t - T_{s,E5}/4\right)\right] \\ & + \frac{1}{2\sqrt{2}}\left(\bar{e}_{E5a-I}(t) + j\,\bar{e}_{E5a-Q}(t)\right)\left[sc_{E5-P}(t) - j\,sc_{E5-P}\left(t - T_{s,E5}/4\right)\right] \\ & + \frac{1}{2\sqrt{2}}\left(\bar{e}_{E5b-I}(t) + j\,\bar{e}_{E5b-Q}(t)\right)\left[sc_{E5-P}(t) + j\,sc_{E5-P}\left(t - T_{s,E5}/4\right)\right] \end{aligned}$$

Eq. (5),

where

$$\bar{e}_{E5a-I} = e_{E5a-Q}\, e_{E5b-I}\, e_{E5b-Q} \qquad \bar{e}_{E5b-I} = e_{E5b-Q}\, e_{E5a-I}\, e_{E5a-Q}$$
$$\bar{e}_{E5a-Q} = e_{E5a-I}\, e_{E5b-I}\, e_{E5b-Q} \qquad \bar{e}_{E5b-Q} = e_{E5b-I}\, e_{E5a-I}\, e_{E5a-Q}$$

Eq (6).

The digital sub carriers $sc_{E5-S}(t)$ and $sc_{E5-P}(t)$ are illustrated in Figure 8.

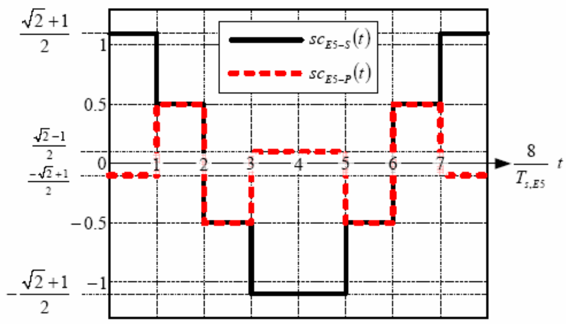

Figure 8: Digital sub carriers of E5 AltBOC signal

Equivalently, the AltBOC complex baseband signal can be described as an 8-Phase Shift Keying (PSK) signal. A PSK signal maintains a constant envelope in the time domain for a balanced signal. The 8-phase constellation is shown in Figure 9.

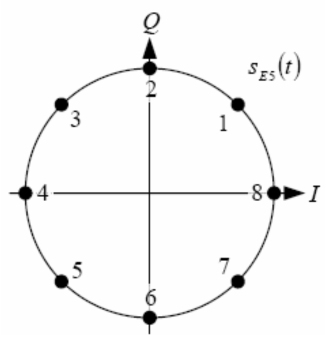

Figure 9: 8-PSK constellation of E5 AltBOC signal

The power spectrum of the simulated Galileo E5 signal is shown in Figure 10. There are two main lobes of width 20*1.023 MHz, and each of these two are centered 15*1.023 MHz away from the center frequency of 1191.795 MHz.

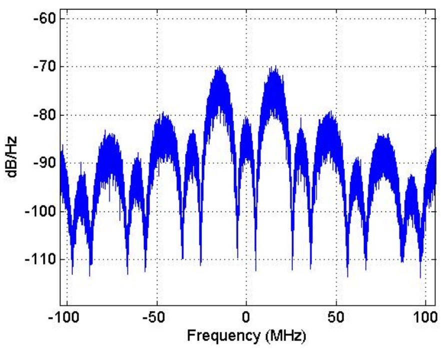

Figure 10: E5 signal power spectrum

The time domain signals with dispersive and non-dispersive ionosphere effect are shown in Figure 11 and 12. As with the study for the E5b signal alone presented earlier, we use TEC=100 TECU for the simulation. The ionosphere disperses the wideband signal to create ripples in the time domain, and transfers part of the original inphase signal to quadrature. This causes a phase change in both the time-domain signal and the correlation peak. It also demonstrates the ionosphere effect on phase. Compared to E5b only signal in Figure 5, the signal distortion due to ionosphere is more pronounced; the time domain ripples have larger amplitude for E5 than for E5b alone. This is because the E5 signal covers wider bandwidth, so the ionosphere dispersion is more significant.

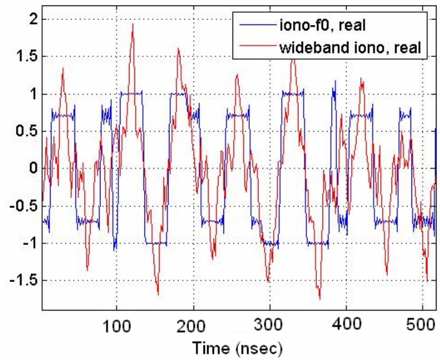

Figure 11: Time-domain E5 signal, real part

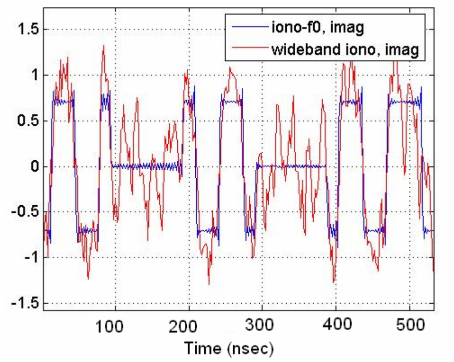

Figure 12: Time-domain E5 signal, imaginary part

The correlation functions are shown in Figure 13. The blue line shows the ideal correlation function without any ionospheric error. The green curve shows the correlation function that might be expected from assuming a nondispersive ionosphere delay at the center frequency. The peak of the green curve is delayed by about 100 ns due to the ionosphere. The red curve shows the real part and the cyan line the imaginary part of the correlation function, which results from including the dispersive effect within the E5 band. In addition to the 100 ns delay relative to the blue ionosphere-free curve, there are two additional features. First, the dispersive ionosphere reduces the correlation peak. Although the ionosphere is not causing a signal power loss at the antenna, there is a correlation power loss with respect to the replica. The norm of the complex correlation function at its peak does not equal 1. In this example, the power loss of the correlation peak is 2.3 dB. Second, the dispersive ionosphere creates an imaginary part in the correlation function, while the signal correlation function with non-dispersive ionosphere has no imaginary part. This would cause a phase shift at the PLL output. In this case, the phase shift is 19.8 degree.

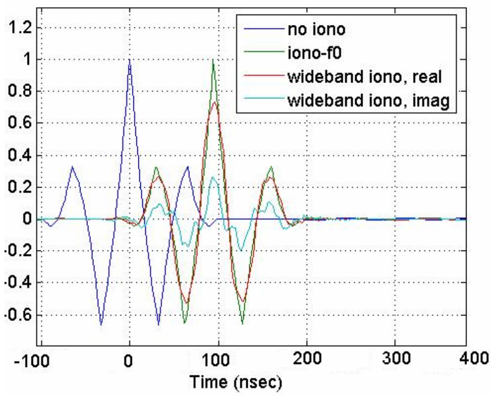

Figure 13: Correlation function of the E5 AltBOC signal for dispersion through 100 TECU ionosphere.

We have set the TEC value to 100 TECU for our simulation so far. Next, we apply different TEC values from 0 to 1000 TECU to obtain the correlation power loss and the phase change under different ionosphere condition. Figure 14 shows the correlation functions for TEC of 150 TECU (a), and 200 TECU (b). The blue curve shows the correlation function that might be expected from assuming a nondispersive ionosphere delay at the center frequency. The green curve shows the real part and the red curve is the imaginary part of the correlation function, which results from including the dispersive effect within the E5 band. Again, the correlation peaks are attenuated due to the ionosphere. In addition to the correlation power loss, there is also phase change at the PLL output. Moreover, as the TEC value goes higher, the correlation peak becomes asymmetric. Take TEC=200 TECU as an example; the imaginary peak of the correlation peak as shown in Figure 14(b) is no longer in the middle, but shifted left.

The dispersive ionosphere has a non-negligible impact on the receiver acquisition and tracking of the Galileo E5 signal. To obtain greater accuracy, Galileo E5 receiver design should compensate the phase change at the PLL output.

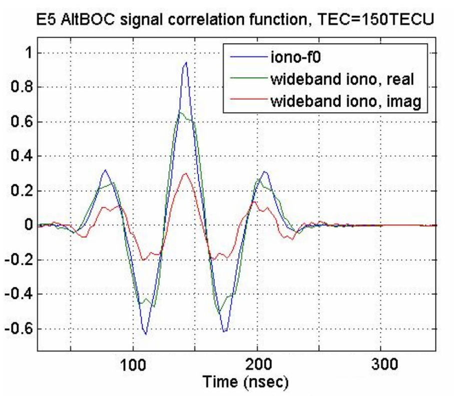

(a) TEC=150 TECU

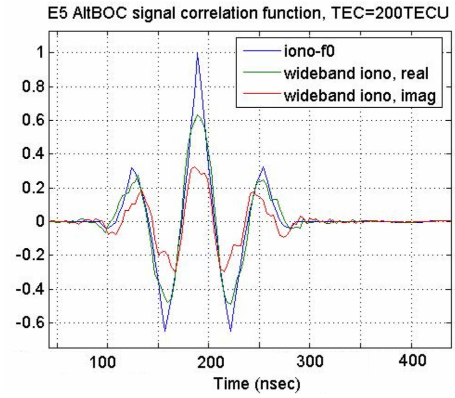

(b) TEC=200 TECU

Figure 14: Correlation function of the E5 AltBOC signal with different TEC values

Figure 15 and 16 show the simulation results of correlation power loss in dB and phase error at the PLL in degrees as a function of TEC from 0 to 1000 TECU. Typical midlatitude nighttime values of TEC range from 0 to 30 TECU. Daytime values may reach up to 250 TECU. TEC values larger than 250 TECU are more likely to be seen during ionospherically active periods.

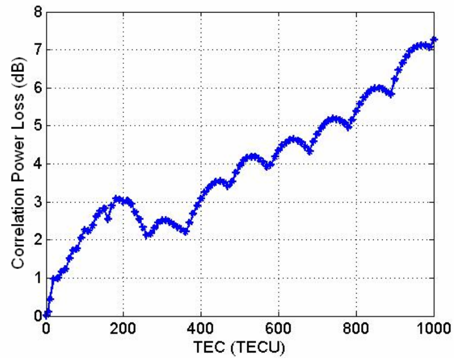

Figure 15: Correlation power loss of the E5 signal correlation peak

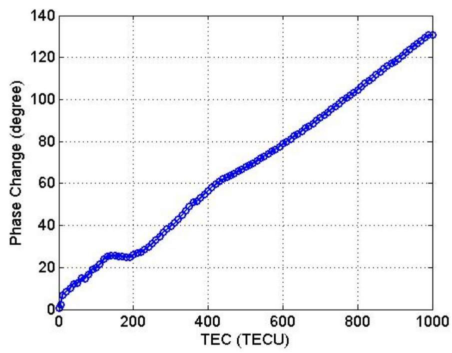

Figure 16: Phase shift at the PLL output

In general, the correlation power loss and the phase change increase as the TEC value increases. This is to be expected, since the ionosphere delay at a given frequency scales with TECU. However, the correlation power loss does not simply increase monotonically, because of the correlation function asymmetry.

SIMULATED WIDEBAND BPSK SIGNALS

In the previous section, we presented the wideband ionosphere effect for the Galileo E5 AltBOC signal with different TEC values. In this section, we will study the impact of varying bandwidth. BPSK signals are used for the simulation since they are simpler and more general than AltBOC signals.

We start from the BPSK signal in the Galileo E5 band. The baseband frequency spectrum is shown in Figure 17. The BPSK signal has a bandwidth of 50 MHz, centered at 1191.795 MHz, the same as the Galileo E5 bandwidth. In contrast to the split spectrum of AltBOC, the spectrum of the BPSK signal has a main spectrum lobe in the middle.

Figure 18 shows the time-domain signals for a dispersive and non-dispersive ionosphere of 100 TECU. The blue curve shows the time-domain signal that might be expected from assuming a nondispersive ionosphere delay at the center frequency. The green curve shows the real part and the red curve is the imaginary part of the time-domain signal with dispersive ionospheric effect. Again, there are ripples in the time domain signal. Compared to the Galileo E5 AltBOC signal in Figure 11 and 12, the amplitude of these ripples are lower, indicating that signal distortion due to the ionosphere is less dramatic. This is because the BPSK spectrum is more centralized than the AltBOC spectrum.

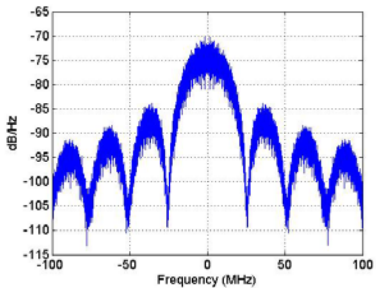

Figure 17: Frequency spectrum of the 50 MHz BPSK signal

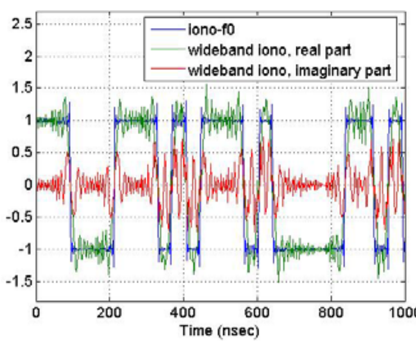

Figure 18: Time-domain 50 MHz BPSK signal

The correlation functions for the 50 MHz BPSK signal are shown in Figure 19. The blue curve and the green curve show the real and imaginary part of the correlation function assuming a nondispersive ionosphere delay at the center frequency. The red and cyan curves show the real and the imaginary part of the correlation function with dispersive ionospheric effect respectively. The correlation peak is reduced by 0.9 dB. The phase change due to ionosphere is 6.4 degrees. Recall that the E5 AltBOC signal at the same center frequency with the same bandwidth suffers the correlation power loss of 2.3 dB and phase change of 19.8 degrees. This demonstrates that a centralized spectrum is more robust to ionosphere degradation.

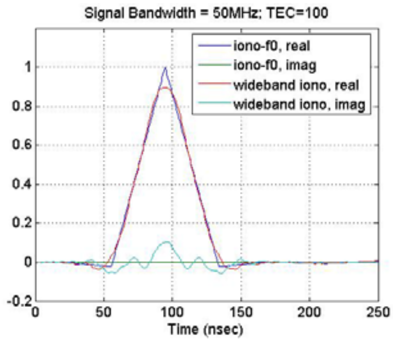

Figure 19: Correlation functions of 50 MHz BPSK signal

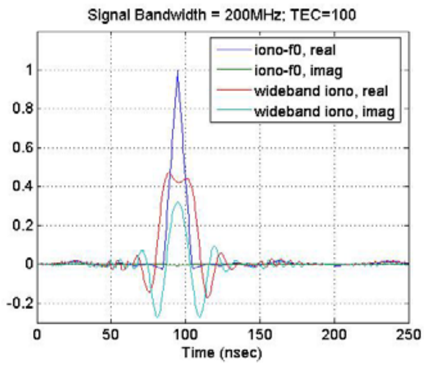

(a) Bandwidth=200MHz

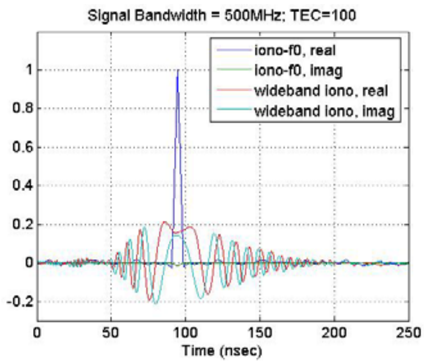

(b) Bandwidth=500 MHz

Figure 20: Correlation functions of BPSK signals with different bandwidths

In addition to the E5 bandwidth, the BPSK signals with ionosphere effect are simulated with different bandwidths. Figure 20 shows the correlation functions for 200 MHz and 500 MHz bandwidth signals traveling through 100 TECU of electrons in the ionosphere. The legend is the same as that in Figure 19. As the bandwidth gets wider, the correlation function gets wider and more sinusoidal. The real part of the correlation peak becomes bimodal and the correlation function asymmetry is more noticeable. Moreover, the correlation peak is attenuated more with wider bandwidth. A more rounded, wider correlation peak implies that narrow correlators will have difficulty tracking for wider bandwidth. When the bandwidth reaches a certain level, for example in Figure 20(b), there will be too many side peaks and no main peak. This would cause failure in both acquisition and tracking

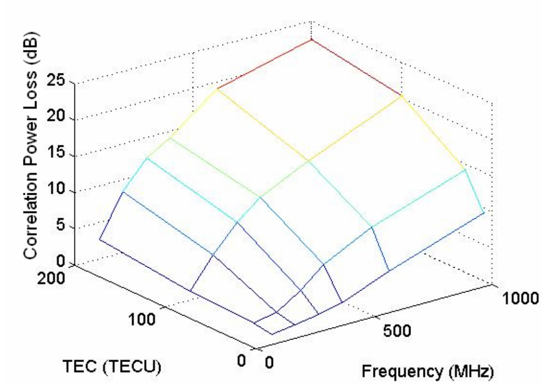

Figure 21: Correlation power loss with different bandwidths and TEC values

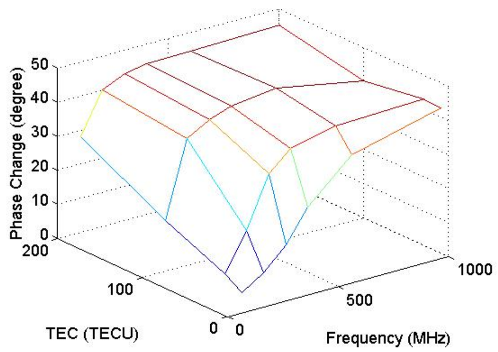

Figure 22: Phase change with different bandwidths and TEC values

The correlation power loss and the phase change with different bandwidth and different TEC values are shown in Figures 21 and 22. The correlation power loss increases with bandwidth and TEC value. If the power loss is greater than 10 dB, the correlation peak would be too weak to track. This defines a safe operating region for bandwidth and TEC value combinations. Beyond this region, receivers would have difficulty in tracking and positioning. The current widest signal bandwidth for the Galileo system is 51 MHz, which is narrow enough that the tracking loops in the receivers would likely converge, based on Figures 21 and 22.

CONCLUSION

This paper shows the ionospheric effects on various wideband GNSS signals: the Galileo E5b signal, the Galileo E5 signal and BPSK signals with different bandwidths. In addition to the group delay and the carrier advance, the ionosphere has extra effects for wideband signals. If wideband ionosphere compensation techniques in receivers are not implemented, the ionosphere causes power loss of the correlation peak, phase change in the PLL output, ripples in the time-domain signals, and correlation peak asymmetry. It has no impact on spectrum shape. The wider the bandwidth and the greater the TEC value, the more dramatic the ionosphere impact is. For the Galileo E5b signal, the chip rate is only 10 MHz, which is not wide enough to make the wideband ionosphere effect significant. However, the Galileo E5 signal has the bandwidth of 51 MHz, and typical ionosphere electron content results in a correlation peak reduction of around 2.3 dB and 19.8 degrees phase error. In order to gain more accuracy, it is suggested the receiver tracking loops compensate the phase change at the PLL output caused by the wideband ionosphere. Other compensation techniques, for example all-pass filtering or iterative TEC estimation, should be applied before the signal is acquired and tracked. Finally, ultra-wideband signals are not recommended for future GNSS signals unless the band is divided into narrower subbands or the received signals are conditioned by mitigating the wideband ionosphere effect.

ACKNOWLEDGEMENT

The authors gratefully acknowledge the support of the Federal Aviation Administration under Cooperative Agreement 95-G-005. This paper contains the personal comments and beliefs of the authors, and does not necessarily represent the opinion of any other person or organization.

REFERENCES

[1] European Space Agency and Galileo Joint Undertaking, ‘Galileo Open Service Signal In Space Interference Control Document (OS SIS ICD)’, Feb 3, 2007. Document can be found on-line at: http://www.galileoju.com/page2.cfm

[2] Christie, Jock R. I., Bradford W. Parkinson, Per K. Enge, ‘The Effect of the Ionosphere and C/A Frequency on GPS Signal Shape: Considerations for GNSS2’,

Proceedings of ION GPS-96 in Kansas City, MO, September 1996

[3] Pratap Misra and Per K Enge, ‘Global Positioning Systems: Signals, Measurements and Performance’, Second Edition, 2006

[4] Grace Xingxin Gao, David S. De Lorenzo, Alan Chen, Sherman C. Lo, Dennis M. Akos, Todd Walter and Per Enge, 'Galileo GIOVE-A Broadcast E5 Codes and their Application to Acquisition and Tracking', ION National Technical Meeting, January 2007, San Diego, CA, USA

[5] M. Soellner and P. Erhard, ‘Comparison of AWGN code tracking accuracy for Alternative-BOC, Complex-LOC and Complex-BOC modulation options in Galileo E5-Band’, The ENC GNSS 2003, Graz, Austria, April 2003